Heuristic structural optimization of 2D filling materials with square-triangular supercells

Eugenio Dragoni

Department of Sciences and Methods for Engineering
University of Modena and Reggio Emilia, Italy
E-mail: eugenio.dragoni@unimore.it

Abstract

Cellular filling materials are a commonplace in additively manufactured parts to lower the structural weight without detriment to the mechanical properties. This technical note undergoes the heuristic optimization of a 2D metamaterial with repetitive supercells derived from a square frame divided by median and diagonal lines into eight triangles. The inherent quadriaxiality of this layout is ideally suited to resist multiaxial stress fields, while enabling size refinement to match the local scale of the component. A step-by-step procedure is developed which optimizes the thickness of the beams along the principal axes of the cell (sidewise and diagonal) according to a fully stressed design concept. Preliminary Finite Element models, including either bar or beam elements, confirm the theoretical results for a case study. Extension of the optimal approach to 3D geometries is envisioned using a cubic cell which incorporates the present 2D grid on each face of the cube.

Keywords

Cellular material, lightweight filling, design, strength, optimization

Introduction

Additive manufacturing of structural machinery parts allows overall weight reductions to be achieved by systematic use of cellular filling materials[1,2]. The outer surface of the part is normally continuous (solid wall, plate, shell etc.) and carries the external loads. The lightweight cellular material fills the internal volumes with the double aim to sustain the localized forces on the surface and distribute the global stresses.

Filling materials are available in many architectures[3]. Very broadly, they can be divided into two categories: materials with flexural behaviour[3-5] (i.e. hexagonal or square cells in 2D, cubic cells in 3D) and materials with membrane behaviour (i.e. triangular cells in 2D, tetrahedral cells in 3D). Materials with membrane behaviour are to be preferred for lightweight applications due to their superior structural efficiency[3]. Instances of this design principle are found in sandwich structures and trabecular bone.

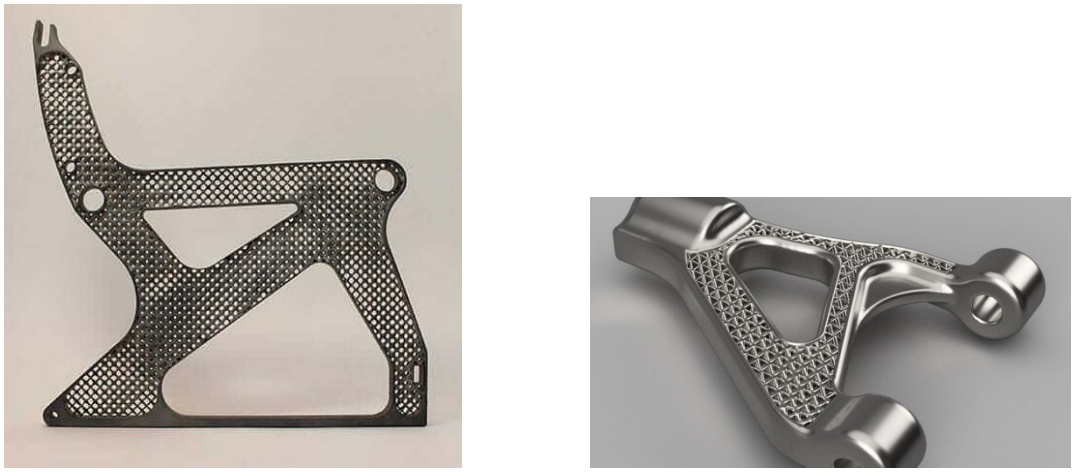

(a) (b)

Figure 1. Use of 2D filling materials in genuine 2D structures (a) and 3D geometries (b) undergoing in-plane loading.

This technical note focuses on the structural optimization of 2D cellular materials subjected exclusively (or mainly) to in-plane loading (Fig. 1). The cell geometry taken into consideration is loosely inspired by the panel framework forming the side girders of the renowned Bailey bridge[6]. As shown in Fig. 2a, it includes an outer square of side $2a$, which is divided by means of two median and two diagonal lines into eight right-angled isosceles triangular cells. The resulting geometry is a redundant lattice structure (which represents the unit cell of the periodic metamaterial) with dominant membrane response under in-plane loading. Advantages of this architecture are the straightforward size gradation of the pattern (Fig. 2b) and the intrinsic quadriaxiality, which facilitates the structural optimization against multiaxial stresses. Published work[7] supplies the macroscopic properties of the unit cell in Fig. 2a by assuming that all beams of the grillage are made from any homogeneous, isotropic material and that they feature the same thickness. The present paper forgoes the latter geometric limitation to pursue a fully stressed state of the beams under assigned global stresses. Design variables are the in-plane thicknesses of the beams, namely: s_1 for the set of horizontal beams, s_2 for the set of vertical beams and s_d for the set of diagonal beams (see Fig. 2a).

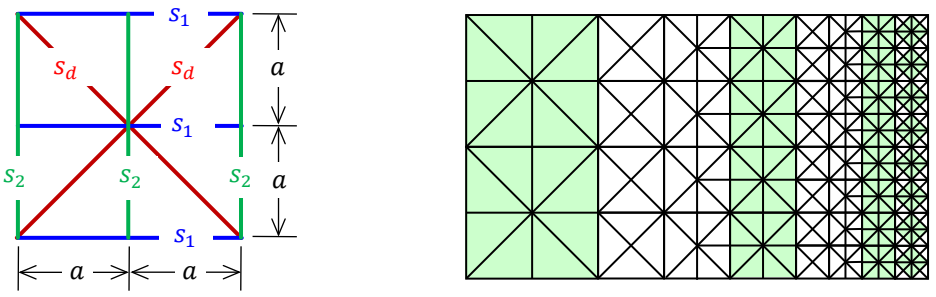

(a) (b)

Figure 2. Geometry of the unit pattern (a) with example of mesh refinement (b), in which the complete unit cells are highlighted in green and the white cells are transition areas.

Optimization

The optimization process refers to the periodic material with the unit cell shown in Fig. 2a repeated indefinitely. For large areas with variable cell size as in Fig. 2b, the procedure must be applied separately for the different regions where the size is constant. Assuming, further, that the members of the unit grid behave either as tension rods or compressive struts, the optimization process is broken down into seven steps as follows.

The first step is the acquisition of the global state of stress to which the cellular filling material is exposed with reference to convenient cartesian coordinates *x-y*

$$\sigma_x, \sigma_y, \tau_{xy} \tag{1}$$

The second step is the computation of principal directions (ϕ_1, ϕ_2) and principal stresses (σ_1, σ_2), based on the well-known relationships of the mechanics of solids

$$\begin{aligned} &\phi_1 = \frac{1}{2}\text{atan2}\frac{2\tau_{xy}}{\sigma_x - \sigma_y} \qquad \phi_2 = \phi_1 + \pi/2 \\ &\sigma_1 = \sigma_m + \tau_{max} \qquad\qquad \sigma_2 = \sigma_m - \tau_{max} \end{aligned} \tag{2}$$

where σ_m e τ_{max} are the normal and tangential stresses, respectively, acting on material planes inclined to $\pm 45°$ with respect to the direction of σ_1

$$\sigma_m = \frac{\sigma_x + \sigma_y}{2} \qquad\qquad \tau_{max} = \frac{1}{2}\sqrt{\left(\sigma_x - \sigma_y\right)^2 + 4\tau_{xy}^2} \tag{3}$$

The third step involves the alignment of the natural directions of the material with the principal stress directions as sown in Fig. 3.

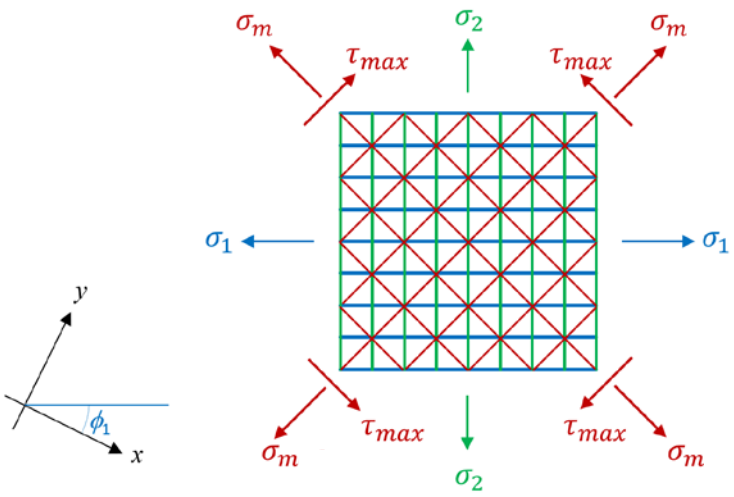

Figure 3. Conceptual alignment of the material with the principal stress directions.

In the fourth step, the scale of the grid (dimension a in Fig. 2) is chosen, together with the base material (virgin polymer, reinforced polymer, metal, …) and its mechanical properties: tensile strength, $\sigma_{adm\,t}$, compression strength, $\sigma_{adm\,c}$, elastic modulus, E.

From the fifth to the seventh step, the optimal thicknesses s_1, s_2 and s_d of the beams in the directions of σ_1 (coloured blue in Fig. 3), σ_2 (coloured green in Fig. 3) and σ_m (coloured red in Fig. 3) are calculated by requesting the full exploitation of the material (fully stressed design). For example, for the horizontal beams in Fig. 3, which are subjected to the tensile stress σ_1, the following equilibrium equation must hold

$$\sigma_{adm\,t}\left(\frac{1}{2}s_1 + s_1 + \frac{1}{2}s_1\right) = \sigma_1(2a) \tag{4}$$

from which

$$s_1 = a\left(\frac{\sigma_1}{\sigma_{adm\,t}}\right) \tag{5}$$

If stress σ_1 were compressive (i.e. negative), Eq. (4) would read

$$\sigma_{adm\,c}\left(\tfrac{1}{2}s_1 + s_1 + \tfrac{1}{2}s_1\right) = -\sigma_1(2a) \tag{6}$$

from which

$$s_1 = -a\left(\frac{\sigma_1}{\sigma_{adm\,c}}\right) \tag{7}$$

For σ_1 compressive, there is also the risk of buckling of the beams. Assuming, conservatively, that both ends are hinged, the magnitude of critical load of the single horizontal beam (of length a) in Fig. 3 is[8]

$$F_{cr} = \frac{\pi^2 E s_1^3}{12a^2} \tag{8}$$

The magnitude of the compressive force is (see Eq. (4))

$$F = -\sigma_1 a \tag{9}$$

By equating (8) and (9) the minimum thickness that prevents buckling of the beam is calculated as

$$s_1 = -a\left(\frac{12}{\pi}\frac{\sigma_1}{E}\right)^{\frac{1}{3}} \tag{10}$$

Finally, introducing a minimum thickness of 10% of a ($= 0.1a$) for manufacturing reasons, the optimal thickness of the horizontal beams is selected as the maximum value between 0.1 a and Eqs. (5), (7), (10). Symbolically

$$s_1 = a \cdot \mathrm{MAX}\left\{0.1\,, \frac{\sigma_1}{\sigma_{adm\,t}}\,, -\frac{\sigma_1}{\sigma_{adm\,c}}\,, -\left(\frac{12}{\pi}\frac{\sigma_1}{E}\right)^{\frac{1}{3}}\right\} \tag{11}$$

If the same reasoning is applied to the directions of σ_2 (vertical in Fig. 3) and of σ_m (diagonal), the following result is obtained

$$s_2 = a \cdot \mathrm{MAX}\left\{0.1\,, \frac{\sigma_2}{\sigma_{adm\,t}}\,, -\frac{\sigma_2}{\sigma_{am\,c}}\,, -\left(\frac{12}{\pi}\frac{\sigma_2}{E}\right)^{\frac{1}{3}}\right\} \tag{12}$$

$$s_d = a\sqrt{2} \cdot \mathrm{MAX}\left\{0.1\,, \frac{\sigma_m}{\sigma_{adm\,t}}\,, -\frac{\sigma_m}{\sigma_{adm\,c}}\,, -\left(\frac{12}{\pi}\frac{\sigma_m}{E}\right)^{\frac{1}{3}}\right\} \tag{13}$$

Note that Eq. (13) does not contain the shear stress, τ_{max}. This is because it is assumed that this stress component is taken care of by the beams of thickness s_1 and s_2, once designed according to Eqs. (11) and (12).

Numerical example

For $\sigma_x = 5$ MPa , $\sigma_y = -8$ MPa , $\tau_{xy} = 3$ MPa, Eqs. (2) and (3) give $\phi_1 = 32.6°, \phi_2 = 22.6°$, $\sigma_m = -1.50$ MPa, $\tau_{max} = 7.16$ MPa, $\sigma_1 = 5.66$ MPa, $\sigma_2 = -8.66$ MPa.

Assuming $a = 10$ mm (Fig. 2a) and adopting as base material a spool of polylactic acid (PLA) with mechanical properties typical of the Fused Filament Fabrication (FFF)

technology[9] ($\sigma_{adm\,t} = 20$ MPa, $\sigma_{adm\,c} = 25$ MPa, $E = 3550$ MPa), Eqs. (11-13) give the optimal thicknesses as: $s_1 = 2.83$ mm (from the second term in Eq. (11)), $s_2 = 3.46$ mm (from the third term in Eq. (12)), $s_d = 1.66$ mm (from the fourth term in Eq. (13)). The resulting framework is shown with reduced scale in Fig. 4a (the thickness normal to the plane of the figure is arbitrary).

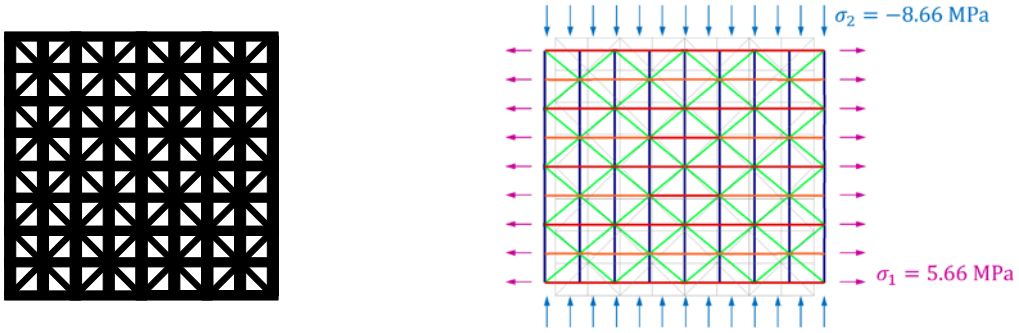

(a) (b)

Figure 4. Final grid of the optimized material (a) with corresponding FE model (b).

Finite Element validation

The grid in Fig. 4a was modelled with 2D bars (beams with end hinges) with cross-section having unit height (normal to the plane of the grid) and thicknesses corresponding to the optimal values of the previous Section. The elastic modulus was $E = 3550$ MPa as before. Figure 4b superimposes the undeformed mesh (grey lines) to the displaced mesh (coloured lines) resulting from the application of the principal stresses calculated above ($\sigma_1 = 5.66$ MPa, $\sigma_2 = -8.66$ MPa). Table 1 compares the FE stresses with the theoretical predictions, showing close agreement. The main difference involves the diagonal beams, where the theoretical stresses exceed their numerical counterparts. This is due to the redundancy of the quadriaxial grid, not included in the theory, which leads to a conservative design (thickness s_d somewhat larger than strictly needed). A run of the

model for the same geometry, material and applied stresses was performed by replacing the hinged bars with proper beams (featuring end rigid nodes). The results were mostly unchanged from Table 1, which confirms that the behaviour of the structure is regulated by membrane action of the beams (i.e. undergoing almost purely axial loading).

Table 1 Theoretical and numerical stresses (MPa) for the optimized material in Fig. 4

Model	Horizontal beams	Vertical beams	Diagonal beams
Theory	+20.0	−25.0	−12.8
FE	+20.4 / +20.8	−24.5 / −24.8	−1.8 / −2.6

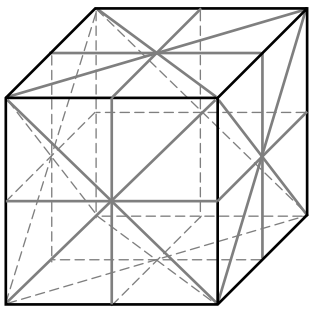

Figure 5. Conceptual extension of the present grid geometry to 3D applications.

Conclusions

The square-triangular supercell studied in this note shows great versatility as 2D lightweight filling material for additively manufactured parts. The layout is easily scaled to match the local geometric features of the component. The intrinsic quadriaxiality of the pattern allows the heuristic optimization of the beam thicknesses according to the fully stressed design criterion. Preliminary Finite Element results, based either on bar or beam

elements, agree with the theoretical predictions for a case study. The research will proceed according to the following lines: 1) systematic testing of the theory by means of parametric 2D Finite Element analyses; 2) experimental validation against physical models; 3) extension of the optimal approach to 3D designs (e.g. the cubic frame in Fig. 5, which incorporates the 2D grid on each face of the cube).

References

1. Kumar A, Verma S and Jeng J-Y. Supportless Lattice Structures for Energy Absorption Fabricated by Fused Deposition Modeling. *3D Printing and Additive Manufacturing* 2020; 7(2): 85–96.

2. Benedetti M, du Plessis A, Ritchie RO, Dallago M, Razavi SMJ and Berto F. Architected cellular materials: A review on their mechanical properties towards fatigue-tolerant design and fabrication. *Materials Science & Engineering R* 2021; 144: 100606 (40 pp).

3. Gibson LJ and Ashby MF. *Cellular materials: structure and properties*. 2nd ed. Cambridge: Cambridge University Press, 1999.

4. Dragoni E and Ciace VA. Mechanical design and modelling of lightweight additively manufactured lattice structures evolved from regular three-dimensional tessellations. *Proc. IMechE, Part C: J. Mechanical Engineering Science* 2021; 235(10), 1759–1773.

5. Ciace VA, Dragoni E and Grasselli L. From three-dimensional tessellations to lightweight filling materials for additively manufactured structures: Concept,

simulation, and testing. *Proc. IMechE, Part L: J. of Materials: Design and Applications* 2022; 236(3), 489–512.

6. Joiner JH. The Story of the Bailey Bridge. *Proc. Inst. Civ. Eng.-Eng. Hist. Herit*. 2011; 164(2), 65–72.

7. Wang A-J and McDowell DL. In-Plane Stiffness and Yield Strength of Periodic Metal Honeycombs. *ASME J. Mater. Engng. Technol* 2004; 126(2): 137–156.

8. Timoshenko SP and Gere JM. *Theory of elastic stability*. 2nd ed. New York: Dover, 1989.

9. Ultimaker, 2022, https://support.ultimaker.com/hc/en-us/articles/360011962720-Ultimaker-PLA-TDS.